Self-propagating thermite reactions: effect of alumina and silica in the starting mixture on the structure of the final products

R. Orrù, B. Simoncini, P. F. Virdis and G. Cao
Dipartimento di Ingegneria Chimica e Materiali - Università degli Studi di Cagliari, Cagliari, Italy

Abstract

The microstructure of the product of the self-propagating thermite reaction between aluminum and ferric oxide varies with the alumina or silica content in the starting mixture. It is shown that corundum, hercynite and iron are always formed regardless the initial alumina content. On the contrary when silica is considered as additive in the starting mixture, mullite and iron are always detected, while hercynite and corundum are found only by decreasing its content to certain levels.

Riassunto

La microstruttura del prodotto finale ottenuto dalla reazione autopropagante di tipo termite fra l'alluminio e l'ossido ferrico dipende dal contenuto di allumina o silice presente nella miscela di partenza.

È possibile osservare che il corindone, l'ercinite ed il ferro si formano indipendentemente dal contenuto iniziale di allumina.

Viceversa, nel caso in cui si impieghi la silice quale addittivo, è stata sempre riscontrata la presenza di mullite e ferro qualunque fosse il contenuto considerato, mentre l'ercinite ed il corindone si formano solo al di sotto di determinati valori critici.

INTRODUCTION

Thermite reactions represent a broad class of highly exothermic reactions, where a metallic or non metallic oxide is reduced by a metal to form a more stable oxide and the corresponding metal or non-metal of the reactant oxide (cf. Wang et al., 1993). Thermite reactions have attracted the attention of researchers and technologists due to their industrial applications such as the pyrotechnic uses (cf. McLain et al., 1980), the synthesis of refractory ceramic and composite materials (cf. Merzhanov, 1990 and reference therein) and the preparation of ceramic linings in metallic pipes (Odawara, 1990; Yin et al., 1993; Chandran et al., 1995; Orrù et al., 1995).

Most of the applications mentioned above are conducted under self-propagating high-temperature synthesis (SHS) conditions, taking advantage of the large values of the heat of reaction which characterizes thermite reactions. SHS represents a technique for the preparation of advanced materials. It is based on the concept that by igniting the starting mixture by means of an external thermal source for relatively short times, a highly exothermic reaction may propagate in the form of a self-sustained combustion wave leading to reaction products progressively without requiring additional energy. This technique represents an attractive alternative to conventional methods of material synthesis due to the simplicity of the process and its relatively low energy requirements, the higher purity of products, the possibility of obtaining complex or metastable phases (cf. Munir and Anselmi-Tamburini, 1989; Varma and Lebrat, 1992; Cao and Morbidelli, 1993; Merzhanov, 1993). It is worth noting that for technological applications additives should be present in the starting mixture in order to reduce the violent character of these reactions. Numerous experimental studies have focused their attention to determine the factors affecting the combustion rate of thermite reactions including particle size of reactants, addition of inert diluents, pre-combustion compact density, salt addition, centrifugal force, ambient inert gas pressure and the physical and chemical stability of oxide reactants (cf. Wang et al., 1993). On the contrary, only little information regarding the microstructure of the product of thermite reactions is available in literature. This basic knowledge not only represents the most important factor which determines the properties of materials (strength, stability, ductility, etc.) but also may be considered as a reference study when investigating the mechanism of structural transformations of thermite reactions. From the pioneering work of Korchagin and Podergin (1979), who studied the interaction of ferric oxide particle on aluminum film using high-temperature diffraction electron microscopy, only recently this type of investigation has received renewed attention. Orrù et al. (1995, 1996, 1997) have studied the mechanism of structure formation of the most representative thermite reaction, i.e. the aluminothermic reduction of ferric oxide, under SHS conditions, in the presence of different alumina and silica content in the starting mixture.

The present study describes the microstructure of the product of the self-propagating thermite reaction between aluminum and hematite by varying the alumina or silica content in the starting mixture from 7 wt% up to 25 wt%. The mechanism of structural transformations of the product resulting from the use of 25 wt% of either alumina or silica is discussed in the other work submitted together with the present one (cf. Orrù et al., 1996).

EXPERIMENTAL SET-UP AND PROCEDURE

The experimental set-up schematically shown in fig. 1 consists of a reaction vessel, a power supply (Belotti, Italy; output 0-100 V) which provides the energy required for reaction ignition, an infrared pyrometer (Land Instrument, Cyclops 152A model), a high-speed video recorder (JVC, AG4700 model), which allows us to record the reaction evolution, and a computer system (Power Macintosh 7200) which not only drives the power supply to produce a well-defined energy pulse but also is equipped with a data acquisition board (Model PCI-MI0-16XE-50, National Instruments) supported by a software package (LabVIEW, National Instruments). A centrifugal mill (Tecnotest, Italy) is used to mix together with acetone, as dispersing agent, reactants and additives in powder form for about six hours. Ferric oxide and aluminum in stoichiometric ratio according to the reaction

$$Fe_2O_3 + 2Al \longrightarrow 2Fe + Al_2O_3$$

and different weight percentage of alumina (7, 18 and 25%) or silica (7, 12, 15, 25%) respectively, were used in powder form (table 1) as received. The obtained mixtures, once dried in air in order to totally eliminate acetone, were then pressed into cylindrical pellets (15 mm in diameter and 20 mm high) in a uniaxial single-acting press (RMU, Italy) at about 10

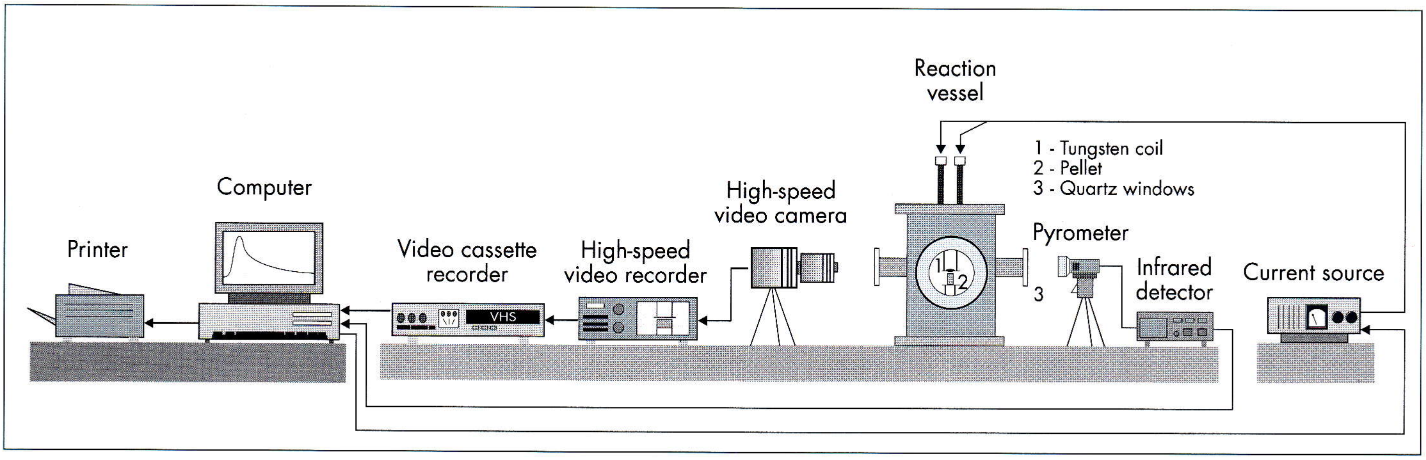

Figure 1: Schematic diagram of the experimental set-up

TABLE 1 - Characteristics of powders

Property	Iron Oxide	Aluminium	Alumina	Silica
Vendor	Aldrich Chem. Co.	Aldrich Chem. Co.	Aldrich Chem. Co.	Aldrich Chem. Co.
Size	< 5 µm	200 mesh avg.	< 10 µm	325 mesh avg
Purity (%)	99 +	99	99.8	99.6

kN for approximately one minute. The green densities of the pellets were determined from weight and geometrical measurements and range from 2.2 to 2.3 g/cm^3 and 2.2 to 2.5 g/cm^3 depending upon the alumina or silica content, respectively. Each pellet was then placed into the vessel and the reaction was initiated at its base by means of a tungsten coil (R.D. Mathis Company, USA) connected to the power supply depicted in fig. 1 which was programmed to produce an energy pulse by setting 20 volts for about 4 seconds. This interval was selected so that the energy source is turned off as soon as the reaction was initiated. The reproducibility of the experimental runs was verified by repeating each of them at least twice.

By combining X-ray diffraction (XRD), optical metallography (OM), scanning electron microscopy (SEM), wavelength and energy dispersive spectroscopy (WDS and EDS) microanalysis, the microstructure of the product was characterized.

RESULTS AND DISCUSSION

As indicated by the videotapes, the melting processes involved are more pronounced when decreasing the percentages of either alumina and silica in the starting mixture. For the case of 25% alumina as additive in the starting mixture, the corresponding XRD pattern is shown in fig. 2. It should be noted that iron peaks are in general rather small due to the fact that, as it will be clearly seen later on, iron is present in the form of small particles that should be eliminated from the sample to be analyzed by XRD. Although the change of alumina content affects the reaction conditions as revealed by the decreasing of the maximum values of the measured combustion temperatures reported in table 2 when increasing its amount, the detected crystalline phases are always corundum, hercynite and iron, and therefore the corresponding XRD patterns are not shown.

The situation substantially changes when adding silica to the starting mixture. This may be clearly seen in fig. 3 - 5 where the XRD patterns corresponding to three different percentages of silica are shown. The observation we made earlier on

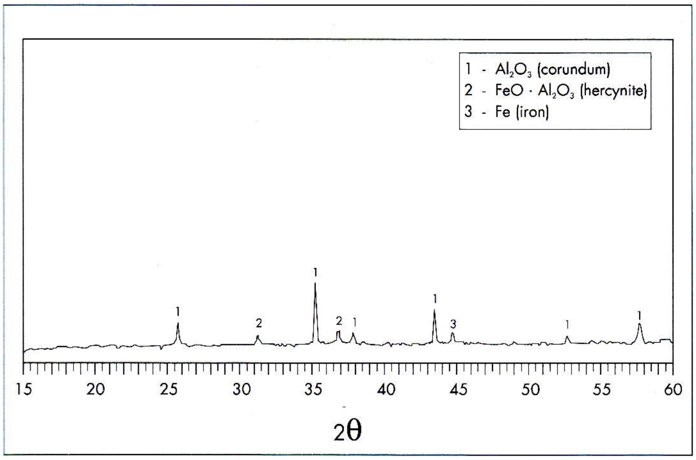

Figure 2: XRD pattern for the case of alumina (25%) as additive

TABLE 2 - Maximum combustion temperatures for the case of alumina as additive

Alumina content (wt%)	7	18	25
T max [K°]	2150	2080	1920

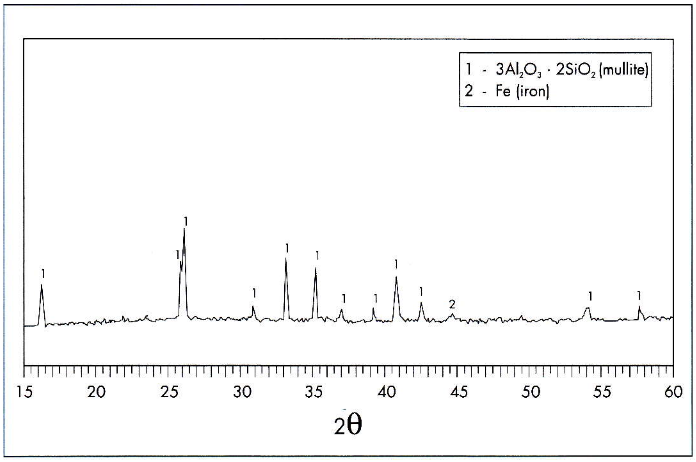

Figure 3: XRD pattern for the case of silica (25%) as additive

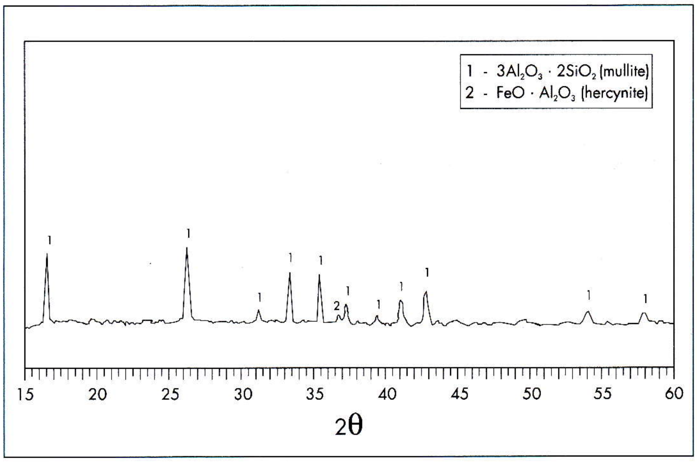

Figure 4: XRD pattern for the case of silica (15%) as additive

the magnitude of iron's peaks can be repeated for these figures. In particular, in fig. 3 - 5 the iron's peaks are so small that are not even indicated. It may be noted that mullite and iron are always revealed regardless the silica content. In particular, these are the only reaction products in crystalline form at 25% of silica. However, as its content decreases, hercynite is found for values of silica equal or lower than 15%, while corundum is detected only at or below 12%.

Also in this case the maximum temperature measured during the course of the reaction decreases by increasing the silica content, as it may be seen in table 3.

After etching with a hydrochloric acid dilute solution, the microstructure of the reacted pellet with 25 wt% of alumina may be seen in the SEM back-scattered micrograph shown in fig. 6. Iron (a), corundum (b) and hercynite (c) are then identified by WDS. Except for the crystal and pore sizes, no variations in the microstructure of the pellets reacted with the other values of alumina content are detected. In particular, crystals and pores become smaller as the alumina content decreases.

The microstructures of the reacted pellets with different silica content are characterized in the following. The corresponding structures were revealed by etching with a hydrofluoric acid dilute solution. A secondary electron SEM view of the microstructure of the sample obtained with 25% of silica is shown in fig. 7.

The corresponding Al-Kα, Si-Kα and Fe-Kα images are reported in fig. 8. Iron (a) and crystalline mullite (b) with different grain size may be clearly seen.

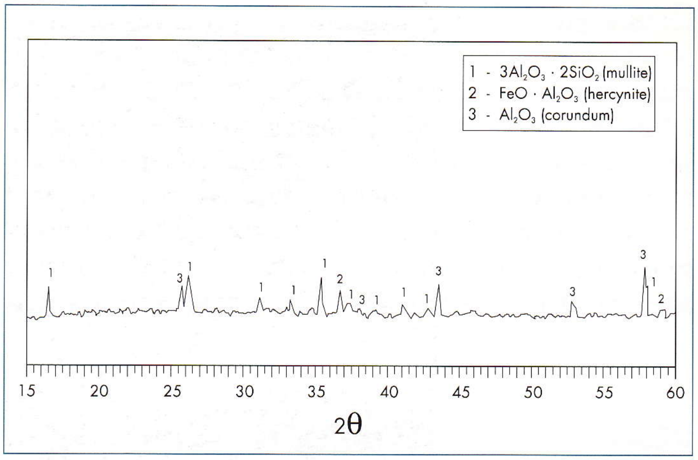

Figure 5: XRD pattern for the case of silica (12%) as additive

TABLE 3 - Maximum combustion temperatures for the case of silica as additive

Silica content (wt%)	7	12	15	25
T max [K°]	2350	2220	2100	1950

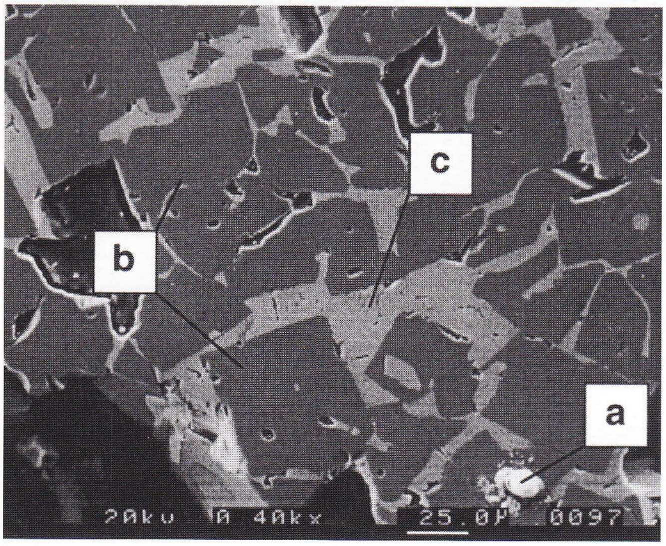

Figure 6: Back-scattered SEM view of the microstructure of the pellet sample reacted with 25% of alumina: iron (a), corundum (b) and hercynite (c)

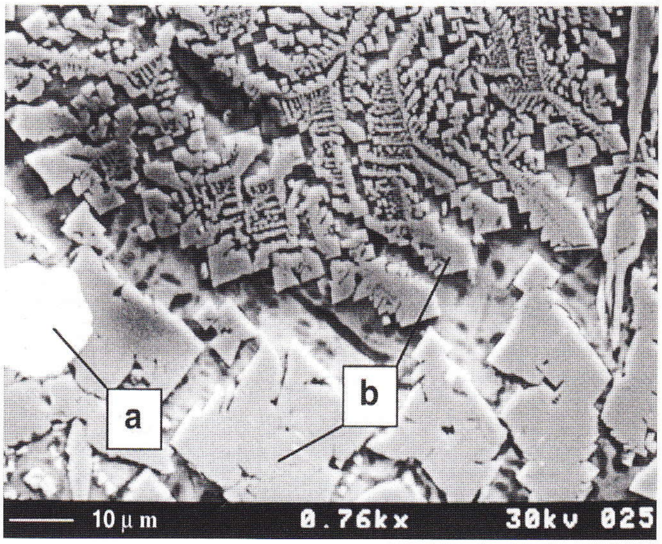

Figure 7: Secondary electron SEM view of the microstructure of the pellet sample reacted with 25% of silica: iron (a) and mullite (b)

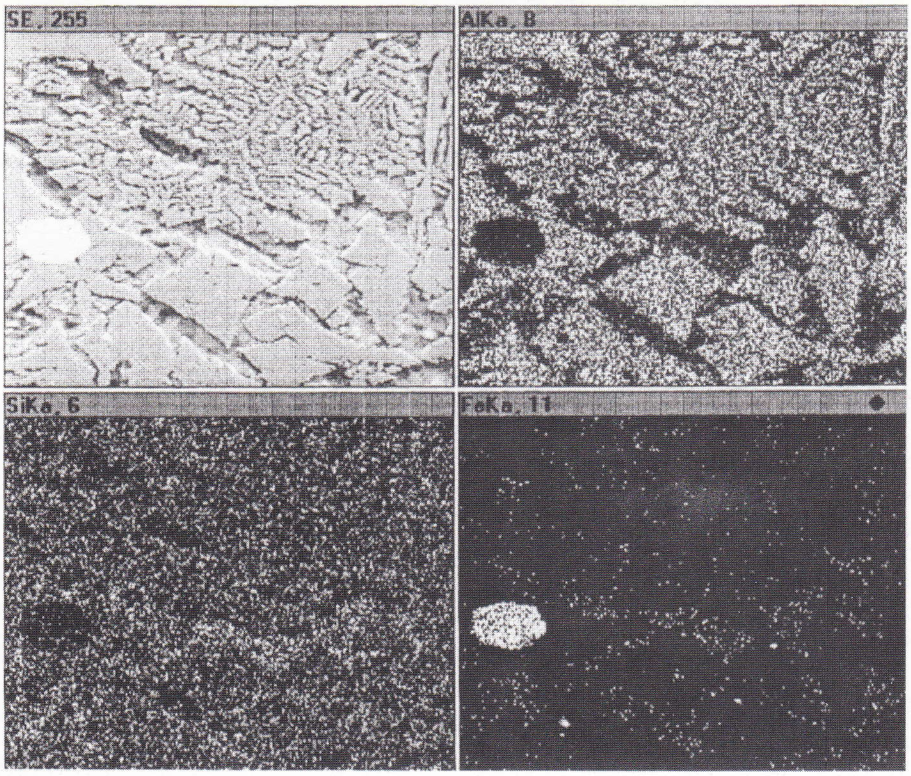

Figure 8: Secondary electron SEM, Fe-Kα, Al-Kα and Si-Kα images of the pellet sample reacted with 25% of silica

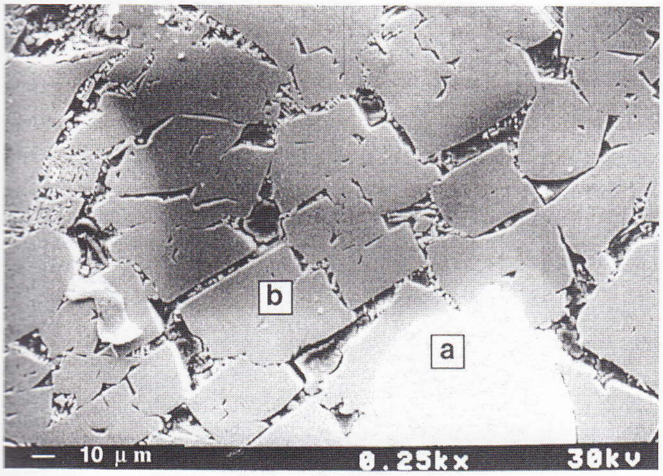

Figure 9: Secondary electron SEM view of the microstructure of the pellet sample reacted with 15% of silica: iron (a) and mullite (b)

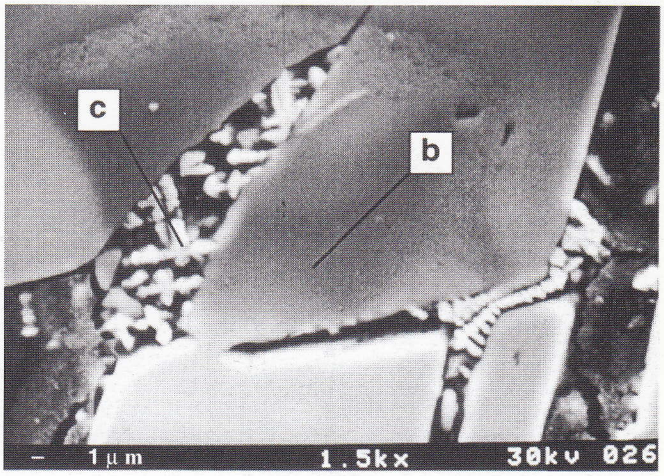

Figure 10: Detailed secondary electron SEM view of Figure 7: mullite (b) and hercynite (c)

The microstructure corresponding to a silica content of 15% is shown in fig. 9. Iron (a) and mullite (b) may be also seen in this case. In addition, at the boundaries of the mullite's crystals the presence of hercynite (c) was revealed as it is apparent from fig. 10 and the corresponding Al-Kα, Si-Kα and Fe-Kα images shown in fig. 11. The resulting microstructure

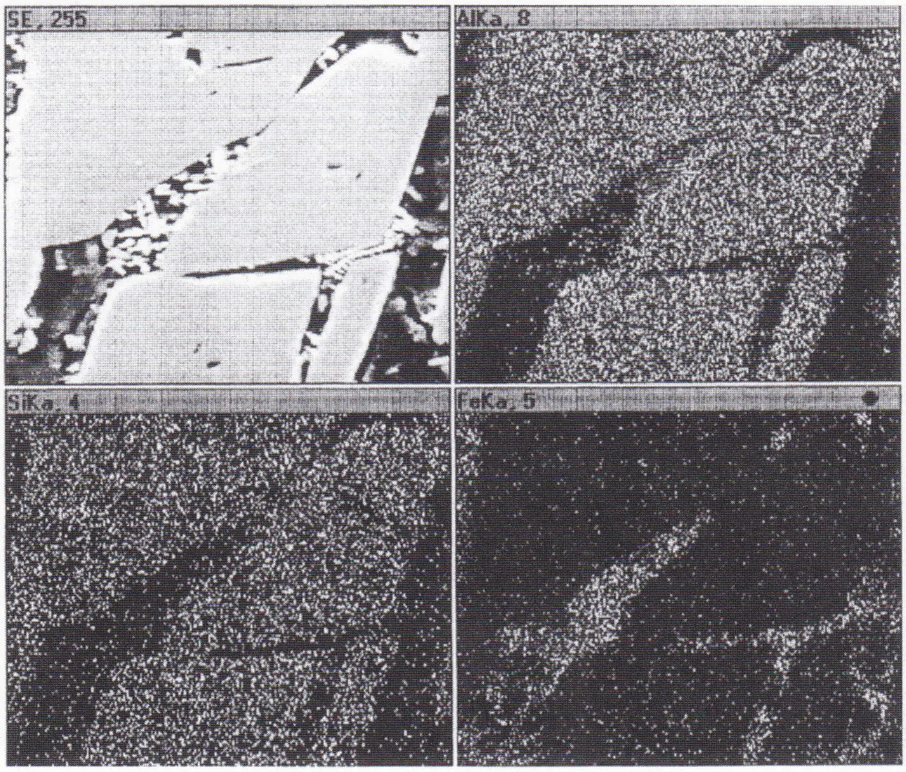

Figure 11: Secondary electron SEM, Fe-Kα, Al-Kα and Si-Kα images of the pellet sample reacted with 15% of silica

with 12% of silica is shown in fig. 12. Apart from the species detected in the previous case, the microstructure changes due to the presence of corundum. A detailed view of the region containing the latter species is shown in fig. 13, whose Al-Kα, Si-Kα and Fe-Kα images are reported in fig. 14. It should be noted that characterization results related to the sample corresponding to the 7% of silica is not reported since only slight changes are found with respect to the case when its content equals 12%.

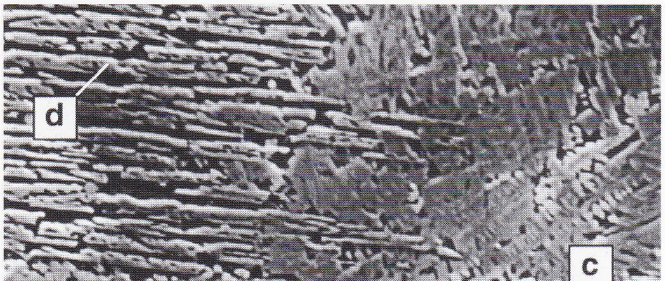

Figure 12: Secondary electron SEM view of the microstructure of the pellet sample reacted with 12% of silica: mullite (b), hercynite (c) and alumina (d)

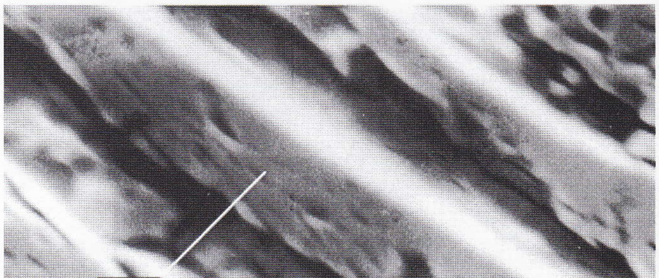

Figure 13: Detailed secondary electron SEM view of Figure 12: alumina (d)

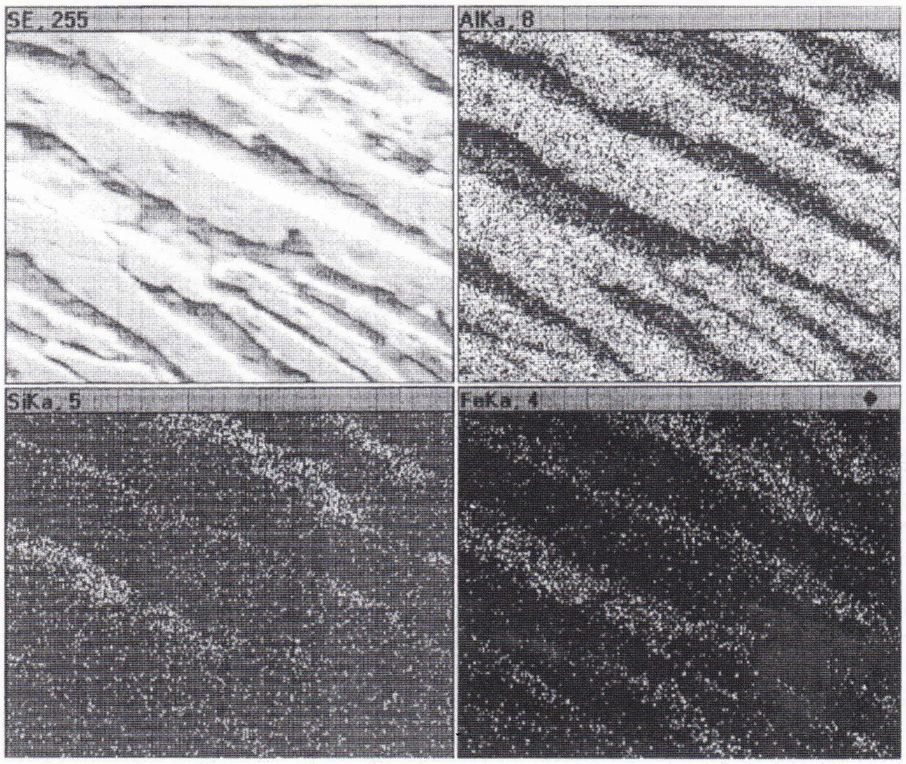

Figure 14: Secondary electron SEM, Fe-Kα, Al-Kα and Si-Kα images of the pellet sample reacted with 12% of silica

CONCLUDING REMARKS

The product obtained from the self-propagating thermite reaction between aluminum and ferric oxide, by varying either alumina or silica content in the starting mixture, is characterized in terms of composition and microstructure. It is found that corundum, hercynite and iron are always formed regardless the variation of the initial alumina content. On the contrary when silica is considered as additive, while corundum and hercynite are found only below a critical value of its content, mullite and iron are always detected.

ACKNOWLEDGEMENTS

We gratefully acknowledge financial support from the Regione Autonoma della Sardegna, Italy.

REFERENCES

1. Cao, G. and M. Morbidelli. Materiali avanzati prodotti per sintesi autopropagante ad alta temperatura. *La Chimica e l'Industria,* 75 (1993), 3-25.
2. Chandran, S., Jagarlamudi, S.K., and J.A. Puszynski. Modeling and experimental studies of simultaneous combustion synthesis and densification in the field of centrifugal forces. In: P. Vincenzini *(Ed.), Proc. of the 8th CIMTEC-World Ceramics Congress and Forum on New Materials - Ceramics: Charting the Future,* Techna Publ., Faenza, 1995, vol. 3C, pp. 2005-2012.
3. Korchagin, M.A., and V.A. Podergin. Investigation of chemical transformations in the combustion of condensed systems. *Comb. Explos. Shock Waves* (Engl. transl.), 15 (1979), 325-329.
4. McLain, J.H. Pyrotechnics: from the viewpoint of solid state chemistry. The Franklin Institute Press, Philadelphia, PA, 1980.
5. Merzhanov, A.G. Self-propagating high-temperature synthesis: twenty years of search and findings. In Z.A. Munir and J.B. Holt (Eds.), *Proc. on Int. Symp. on Combustion and Plasma Synthesis of High Temperature Materials.,* VCH Publishers, New York, 1990, pp. 1-53 .
6. Merzhanov, A.G. Theory and practice of SHS: worldwide state of the art and newest results. *Int.* J. *of SHS,* 2 (1993), 113-158.
7. Munir, Z.A., and U. Anselmi-Tamburini. Self-propagating exothermic reactions: the synthesis of high-temperature materials by combustion. *Mater. Sci. Rep.,* 3 (1989) 277-365.
8. Odawara, O. Long ceramic-lined pipes produced by a centrifugal-thermite process. *J. Am. Ceram. Soc.,* 73 (1990), 629-633.
9. Orrù, R., Simoncini, B., Virdis, P.F., and G. Cao. Further studies on a centrifugal SHS process for coating preparation and structure formation in thermite reactions. *Int. J. of SHS,* 4 (1995), 137-147.
10. Orrù, R., Simoncini, B., Virdis, P.F., and G. Cao. Mechanism of structure formation in self-propagating thermite reactions: comparison between alumina and silica as additives in the starting mixture. *Metallurg. Sci. Tech.,* 14 (1996), 69-77.
11. Orrù, R., Simoncini, B., Virdis, P.F., and G. Cao. Mechanism of structure formation in self-propagating thermite reactions: the case of alumina as diluent. *Chem. Eng. Comm.*, inpress (1997).
12. Varma, A. and J.P. Lebrat. Combustion synthesis of advanced materials. *Chem. Engng. Sci.,* 47 (1992), 2179-2194.
13. Wang, L. L., Munir, Z.A., and Y.M. Maximov. Thermite reactions: their utilization in the synthesis and processing of materials. *J. Mat. Sci.,* 28 (1993), 3693-3708.
14. Yin, S., Liu, M., Yao, C., and Z. Guo. Feldspar additive in ceramic composite pipes made by a centrifugal SHS process. *Int. J. of SHS,* 2 (1993), 69-74.